Concrete Repair, Rehabilitation and Retrofitting II – Alexander et al (eds)
© 2009 Taylor & Francis Group, London, ISBN 978-0-415-46850-3

Debond detection in RC structures using piezoelectric materials

X.Q. Zhu & H. Hao
CRC for Integrated Engineering Asset Management
School of Civil and Resource Engineering, The University of Western Australia, Australia

K.Q. Fan
CRC for Integrated Engineering Asset Management
School of Civil and Resource Engineering, the University of Western Australia, Australia
School of Information Technology, Wuyi University, Guangdong, China

Y. Wang
CRC for Integrated Engineering Asset Management
School of Civil and Resource Engineering, the University of Western Australia, Australia
School of Civil Engineering, Harbin Institute of Technology, China

J.P. Ou
CRC for Integrated Engineering Asset Management
School of Civil Engineering, Harbin Institute of Technology, China

ABSTRACT: This paper presents a technique to detect the delamination between the steel bars and concrete in the reinforced concrete structures. The piezoelectric components are mounted on reinforcing bars that are embedded in RC structures as sensors and actuators to generate and record the signal, which is sensitive to the delamination between the steel bars and concrete. The experimental study is carried out on a concrete slab with different debonds between the rebars and concrete. The test results show that the delamination between the rebars and concrete can be detected with the embedded piezoelectric sensors and actuators.

1 INTRODUCTION

Reinforced concrete (RC) structures are widely used in civil infrastructure systems because of low construction cost and long service life under various conditions. The behaviour of reinforced concrete structures under both static and dynamic loads is highly dependent on the interface between the concrete and the reinforcing bars. When the interface is seriously damaged, such that a macro-crack is formed, debonding takes place and large slip occurs, and the load-transferring capacity of the interface will drop dramatically. A great effort has been made in order to understand the main stress transfer mechanisms between concrete and steel in reinforced concrete elements that are represented by adhesion, mechanical interaction and friction. Neild et al (2002) studied the non-linear behaviour of reinforced concrete beams under low-amplitude cyclic vibration. He outlined four mechanisms which are responsible for the nonlinear vibration characteristics, i.e. crack closure leading to a bilinear stiffness mechanism, friction across the crack due to matrix-aggregate interaction, slip between the steel bar and the concrete and the non-linear behaviour of concrete in compression. The most important one is the bonding damage between the reinforcing bar and the concrete. Soh et al (1999) presented a damage model, which included the normal and tangential damage factors, to describe the concrete-steel interface mechanism. A reinforced concrete element is developed based on this damage model to simulate the bond deterioration in reinforced concrete structures (Soh et al, 2003). Limkatanyu and Spacone (2002) presented the general theoretical framework of the displacement-based, force-based, and mixed formulations of reinforced concrete frame elements with bond slip in the reinforcing bars. Zhu and Law (2007) developed a damaged reinforced concrete beam finite element based on the constitutive law of the lumped model on the concrete-steel interface. Scalar damage parameters characterizing changes in the interface are incorporated into the formulation of the finite

element that is used in the damage identification procedure from static responses.

In recent years, structural health monitoring (SHM) has been increasingly recognized as a viable tool for improving the safety and reliability of structures. Many monitoring techniques have been reported in the literature by Doebling et al (1998). These methods can be generally classified as either global or local. Global approaches are based on relatively low-frequency vibration measurements of the structure. The first few modes are used to assess the locations and the amount of damage. However, a small number of the global modes are not sufficient to detect minor damage in the structure. Also a common limitation of these techniques is that they require a high-fidelity model of the structure to start with. The global approaches are not suitable for the detection of a relatively small damage, especially the delamination or separation of concrete and steel bar at the interface.

Many of conventional non-destructive evaluation (NDT) methods, such as radiography, acoustic emission, magnetic field, eddy-current, thermal field and ultrasonic techniques, are visual or localized methods (Chang and Liu, 2003). All these techniques require that the vicinity of the damage is known a priori and that the portion of the structure being inspected is readily accessible. Recently, guided waves have been widely used for SHM and NDT (Soh et al, 2000; Yan and Yam, 2002; Lee and Sohn, 2006). All elastic waves including body and guided waves are governed by the same set of partial differential equations. The primary difference is that, the body waves are not constrained by any boundaries, but the guided waves need to satisfy the boundary conditions imposed by the physical systems as well as the governing equations (Rose, 1999). Due to this point, the guided waves can propagate a relatively long distance with little attenuation, thus providing a sensing range which is between those of conventional NDT techniques and global SHM techniques.

Piezoelectric materials are widely used for exciting and measuring guided waves in SHM and NDT applications. This material has unique electrical-mechanical characteristics that acting in the "direct" manner produce an electric charge when stressed mechanically, and conversely, a mechanical strain is produced when an electrical field is applied. Due to these characteristics, it has captured increasing interest from both academic and industrial communities to develop the health monitoring technique based on piezoelectric ceramics (Soh et al, 2000; Yan and Yam, 2002; Tseng and Wang, 2004; Lee and Sohn, 2006; Park et al, 2006). There are mainly two types of damage detection strategies based on the piezoelectric elements. Based on the electro-mechanical coupling property of piezoelectric materials, the impedance-based method has been reported for successful applications to damage detection of various types of structures, such as a reinforced bridge (Soh et al, 2000), concrete beams (Tseng and Wang, 2004), steel bridge components (Park et al, 2006). The root-mean-square deviation is used to quantify changes in the impedance signature due to the presence of damage. Another type of methods is the lamb wave-based damage detection technique. Recently, this technique is used to detect the bonding condition between the carbon fiber-reinforced polymer (CFRP) and the host structure (Kim et al, 2007). A reference-free damage diagnosis is achieved based on the concept of time reversal acoustics (TRA). In TRA, an input signal at an excitation point can be reconstructed if the response signal measured at another point is reemitted to the original excitation point after being reversed in time domain. Wu and Chang (2006a & b) presented a pitch-catch method to detect the debond damage in reinforced concrete structures. The changes in the transmission velocity or energy of elastic waves associated with damage are identified using the pitch-catch method. Wu and Chang (2006a) performed an experimental investigation for reinforced concrete structures using built-in piezoelectric discs as sensors and actuators. The test results showed that the amplitude of the received signal increased with the extent of debond and the arrival time is sensitive to the rebar's elongation. The phenomena were delineated using numerical simulations (Wu and Chang, 2006b).

This paper presents a technique to detect the delamination between the steel bars and concrete in the reinforced concrete structures. The piezoelectric components are mounted on reinforcing bars that were embedded in RC structures as sensors and actuators to generate the signal, which is sensitive to the delamination between the steel bars and concrete. The experimental study is carried out on a concrete slab with different debonds between the rebars and concrete. The test results show that the delamination between the rebars and concrete can be detected with the embedded piezoelectric sensors and actuators.

2 THEORETICAL FRAMEWORK

2.1 *Wave selection*

The narrow band windowed sine burst wave is one of the wave types. Because of its narrow band, wave dispersion gets controlled as the wave propagates in a medium. With this type of wave, changes in the waveform could be observed easily. Since the waveform is very sensitive to any anomalies in the wave propagating medium, this wave type has been widely used in structural health monitoring. The waveform of a Morlet wavelet has the finite duration at a specific frequency. It is nothing more than a sine wave multiplied by a Gaussian envelope as follows

$$\psi(t) = Ae^{-\frac{t^2}{2\sigma^2}} e^{-j2\pi ft} \quad (1)$$

where f is the centre wavelet frequency, σ is the bandwidth parameter and j is the imaginary unit. The bandwidth parameter σ controls the shape of the basic wavelet. Here, the wave is generated as the real part

$$\psi(t) = Ae^{-\frac{t^2}{2\sigma^2}} \cos(2\pi ft + \varphi) \quad (2)$$

where φ is the phase. Normally, the waveform is defined in $\pm 3\sigma$, and the number of waves n is $n = 6\sigma f$. 6σ is the time duration of the waveform.

As the above, the waveform is controlled by two parameters: the number of waves n and the wave frequency f. The wave frequency corresponds to the wavelet central frequency and the bandwidth of the waveform is $\sigma = n/6f$. For example, Figure 1 shows the waveforms and their Fourier spectrum when $n = 5, 10, 20$. The sampling frequency is 2 MHz and the wave frequency is 50 kHz. In the figure, the time duration reduces with the decrease of the number of waves, but the frequency bandwidth increases. If the number of waves is selected as 10, the time duration and the frequency bandwidth are about 0.2 ms and 20 kHz, respectively.

2.2 *Wave propagation along steel bars inside or outside of concrete*

In an infinite solid medium, elastic waves can propagate in two basic modes: pressure (P) waves and shear (S) waves. However, wave reflections occur at the boundary between the steel bar and concrete and more complicated wave patterns emerge. The ultrasonic methods relay on elastic wave propagation and reflection with the material. The wave field disturbance due to local damage and flaws is used to identify damages. Therefore, a conventional Lamb wave approach may not be applicable for the monitoring of delamination between the rebars and concrete, a new approach, which can be used regardless of the complexity of waves, is necessary.

Figure 2 shows the wave propagation along a 1600 mm length steel bar (Diameter 10 mm). The frequency of the waves is 50 kHz and the number of the waves is 10. The distance between the actuator and the sensor is 1000 mm. The sampling frequency for data record is 2 MHz. In Figure 3, there is a time difference between the input and output signals. The corresponding time intervals for 3 waves are 0.200 ms, 0.327 ms and 0.433 ms, respectively. The first wave is the incident wave from the input, and the second and third waves are reflecting wave by the two ends of the steel bar. Due to the distance between the actuator and the left end is the same as that between the sensor and the left end. The second wave is a combination

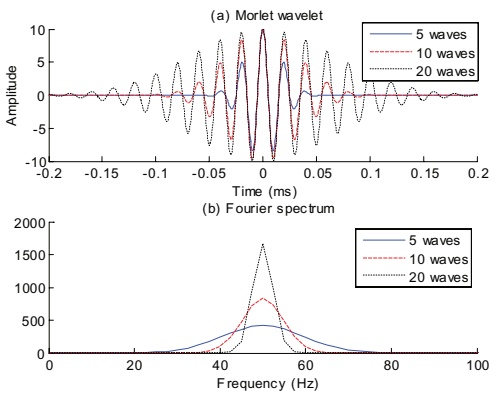

Figure 1. Morlet wavelet and its Fourier spectrum.

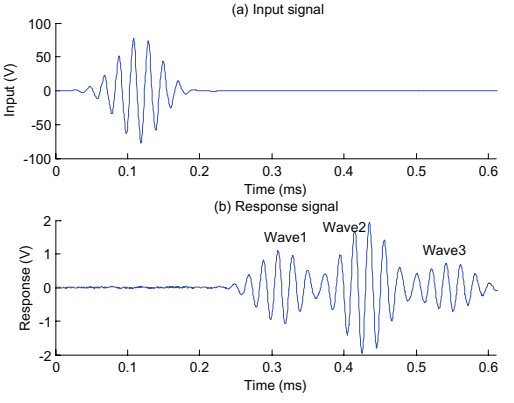

Figure 2. Wave propagation along the steel bar.

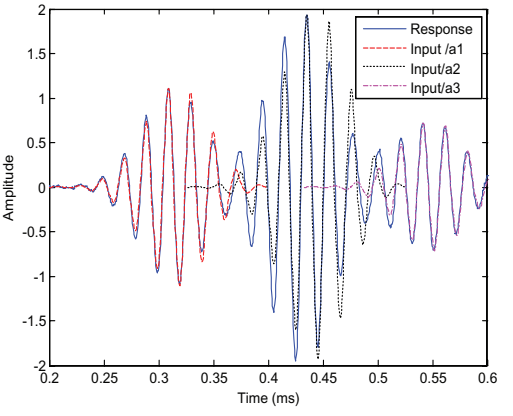

Figure 3. Comparison of the input and output signals by shifting and normalizing.

of the reflected waves from the two ends. The wave propagation distances of these waves from the actuator are 1000 mm, 1600 mm and 2200 mm. So the average wave speeds are 5000 m/s, 4893 m/s and 5081 m/s, respectively. The peak-peak values of the 3 waves are 2.148 V, 3.838 V and 1.406 V, respectively. The value is reduced with the propagation distance except for the second wave. The second wave consists of the two reflected waves from the two ends. This intensifies the wave amplitude. To check if there is any change in wave frequency and wave form, the excitation wave is shifted and normalized to the same amplitude as the incident and reflected waves as shown in Figure 3. The scale factors for the 1st, 2nd and 3rd waves are a1 = 0.144, a2 = 0.252 and a3 = 0.093, respectively. The corresponding shifted times are t1 = 0.200 ms, t2 = 0.327 ms and t3 = 0.433 ms. The results show that both the incident and reflected waves have very similar wave form and wave frequency as the excitation wave.

In order to understand the wave propagation along the steel bar in concrete, the above steel bar is cast into a reinforced concrete beam (1500 mm × 250 mm × 250 mm). The minimum concrete cover is 50 mm. The total steel bar length is the embedded length of 1500 mm in the concrete plus 53 mm overhanging outside of the concrete at the receiving side, and 47 mm on another side. Figure 4 shows the comparison of wave propagation along the steel bar in or out of concrete using the same input signal. The wave frequency is 50 kHz and the number of the waves is 10. For the first wave measured on the bar inside the concrete, there is an arrival time delay of 0.30 ms and an amplitude reduction of 1.4 times as compared with that on the bare steel bar.

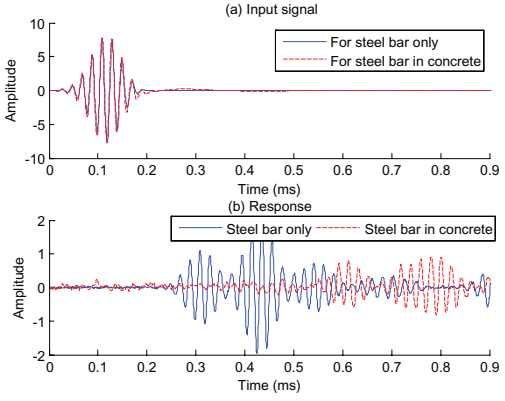

Figure 4. Comparison of wave propagation in or outside of concrete.

2.3 *Damage assessment using changes of the wave speed and amplitude*

As above, two parameters are changed when the wave propagates along the steel bar in or outside of concrete: the wave speed and amplitude. The speed of the wave propagation along the steel bar in concrete are related to the property of the interface between steel bars and concrete. Measurements of the wave speeds using the embedded piezoelectric sensors provide a technique to assess the delamination in the interface. Supposing that the distance between the tip of actuator and the tip of the receiver is L and the time for the wave to travel this distance is t, the average speed of the wave is $v = L/t$. If the wave speeds along a bare steel bar or a bar inside concrete without delamination are v_s and v_c, respectively, the scalar parameter can be defined as follows

$$\alpha_{\text{speed}} = 1 - \frac{v - v_c}{v_s - v_c} \tag{3}$$

where α_{speed} is a scalar parameter. $\alpha_{\text{speed}} = 0$ corresponds to the wave propagation along the bare steel bar and $\alpha_{\text{speed}} = 1$ is for the steel bar in concrete without delamination.

The wave amplitude is another parameter to be affected by the interface between steel bars and concrete. When the wave travels through a medium, its intensity diminishes with the distance. Attenuation that includes the combined effect of wave scattering and energy dissipation is the decay rate of wave as it propagates in a solid. For a single frequency wave, the amplitude change of a decaying plane wave can be expressed as

$$A = A_0 e^{-\alpha x} \tag{4}$$

where A_0 is the amplitude of the wave at the actuating point and A is the reduced amplitude after the wave travelled a distance x from the initial location. α is the attenuation coefficient of the wave travelling in the x-direction.

Similar to the scalar parameter α_{speed}, there is another parameter corresponding to the changes of the wave amplitude

$$\alpha_{\text{amplitude}} = 1 - \frac{A - A_c}{A_s - A_c} \tag{5}$$

where A_s, A_c are the amplitudes of wave propagating along the bare steel bars or in concrete without delamination, respectively. $\alpha_{\text{amplitude}} = 0$ or 1 indicates

that there is no concrete around the steel bar, or the steel bar is in the concrete without delamination in the interface, respectively.

3 EXPERIMENTAL SETUP

To build an active sensing system using embedded piezoelectric components, two sets of experimental tests were performed to highlight the viability to detect the delamination between the rebars and concrete. The first set is to study the mechanism of wave propagation along the steel bar in the concrete and optimize the excitation frequency and time duration of the actuating signal. The second set is the debond tests that were conducted to observe signal changes due to the debond damage in the structure and find the possible candidate of the damage index in the signature.

The experimental system, shown in Figure 5, includes two parts: a) the actuating part is to provide the excitation or input of the system. It includes the actuator of piezoelectric strips and the power amplifier that provides the power supply to the actuator. b) The piezo sensing part is to measure the response. This part includes the piezo film element and its charge amplifier.

The actuators were mounted on the surface of the steel reinforcing bar with Araldite Kit K138 and the steel bars were cast into a concrete slab to evaluate the delamination between the steel bars and concrete. The strip actuators from APC International, Ltd. are selected in this study. The actuator includes two thin strips of piezoelectric ceramic that bonded together, with the direction of polarization coinciding and are electrically connected in parallel. When electrical input is applied, one ceramic layer expands and the other contracts, causing the actuator to flex. In this study, only one ceramic layer is applied with the electrical input so that it will generate the wave. NI USB-6251 is used to provide the short-time Morlet wavelet for actuating the structure by a linear power amplifier. The frequency and the number of waves can be adjusted to optimize the wave propagation along the steel bars.

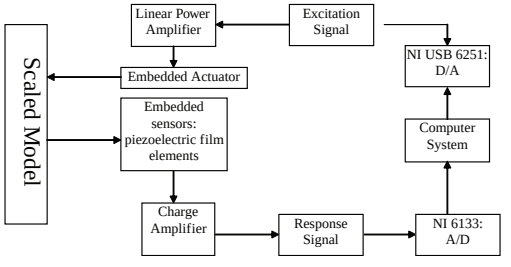

Figure 5. Experimental setup.

The waves have been generated as above by Equation (2). Because wave signals decay quickly in concrete structures, the signal input on the actuators should be as strong as possible to generate readable output at the sensors. A linear power amplifier was developed to amplify the signals from the output of NI USB 6251.

The DT1 series piezo film elements from Measurement Specialties, Inc. are selected as the sensors. The sensors are also glued to the steel bars with Araldite Kit K138. Signals from sensors are collected by a data acquisition system based on NI PCI-6133. The sampling frequency of the system is up to 2 MHz. A program based on Labview is developed to control NI USB-6251 and 2 NI PCI-6133 simultaneously.

A reinforced concrete slab (1500 mm × 500 mm × 100 mm), shown in Figure 7, are constructed for debond tests in the laboratory. The slab is supported at two ends. The slab includes 5 reinforcement bars (round bar with diameter 16 mm) with 50 mm cover of concrete to reduce the effect of the concrete thickness. The distance between two rebars is about 100 mm. The strength of the rebars is 250 MPa. The slab was covered in plastic the following day after pouring the concrete and then the formwork was stripped after 14 days in compliance with the code requirement stated in AS36610 clause 19.6.2.5. Cylinders for the slab were tested after 28 days and had an average compressive strength of 40.2MPa. The Young's modulus of the slab is 3.3×10^{10} Pa and the density is 2450 kg/m^3.

In the slab, there are 5 reinforcement bars with different debond sizes between the reinforcement bar and concrete, b = 0 mm, 21 mm, 37 mm, 58 mm and 99 mm as shown in Figure 6. Debonding is simulated by a plastic tube sealed at two ends so that concrete can not enter the tube during the casting. One actuator and four piezo film elements with different distances (400 mm, 600 mm, 800 mm and 1000 mm) are mounted on the surface of the reinforcement

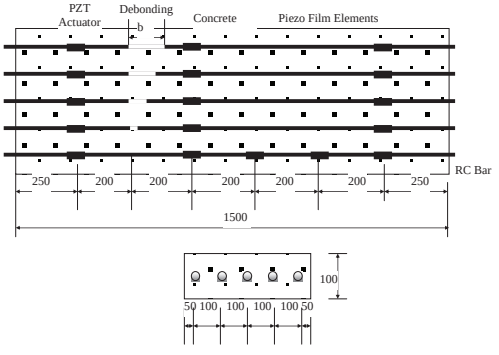

Figure 6. Two concrete slabs for debond tests.

bar without debond, and other rebars are with one actuator and two piezo film elements at 400 mm and 1000 mm, respectively as shown in Figure 6.

4 EXPERIMENTAL RESULTS

Figure 7 shows the time delay and amplitude changes with the exciting frequency. Figure 8 shows wave propagation along the rebars with different debonding lengths. From these results, the following observations can be obtained

1. In Figure 7(a), the time delay remains the same when the exciting frequency is from 30 kHz to 80 kHz and it increases with the sensor number. That means the excitation frequency in the range 30~80 Hz has no effect on the time delay.
2. In Figure 7(b), the amplitude of the response reduces with the excitation frequency.
3. In Figure 8, the time delay of the response signal reduces with the debonding length. Corresponding to the no debonding case, the time delays are 0.401 ms for 37 mm debonding, 0.363 ms for 58 mm debonding. The distance between the actuator and sensor is 1000 mm. From Equation (3), α_{speed} are 0.97, 0.87 for 37 mm and 58 mm debonding, respectively. α_{speed} reduces with the debonding length and it could be a good indicator of the debonding damage.
4. In Figure 8, the amplitude of the response signal increases with the debonding length. The amplitudes for no debonding, 37 mm and 58 mm debonding are 0.063, 0.146 and 0.215, respectively. By Equation (4), $\alpha_{amplitude}$ are 0.84, 0.71 for 37 mm and 58 mm debonding, respectively. $\alpha_{amplitude}$ also reduces with the debonding length, and it could be another indicator of the debonding damage.

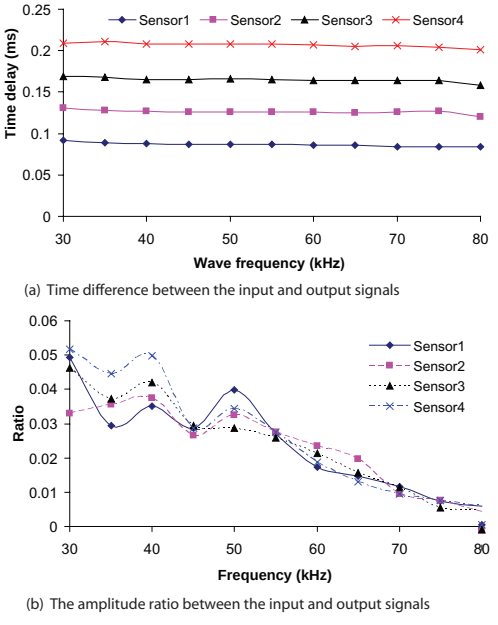

Figure 7. Signal changes with the excitation frequency.

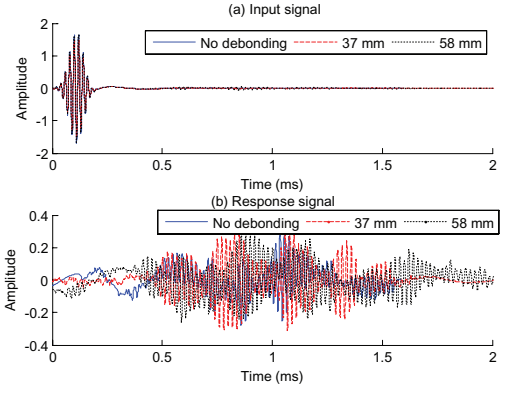

Figure 8. Wave propagation along the rebars with different debond lengths.

5 CONCLUSIONS

A new method has been presented to detect the delamination between the steel bars and concrete in the reinforced concrete structures. The experimental study is carried out on a concrete slab with different debonds between the rebars and concrete. Two scalar parameters are defined according to the changes in the received signal to detect debonding damage. The test results show that they could be good indicators of the debonding damage. Further study is needed to quantify the debonding damage.

ACKNOWLEDGEMENTS

The work described in this paper was supported from CIEAM through Project ID207.

REFERENCES

Chang, P.C. & Liu S.C. 2003. Recent research in nondestructive evaluation of civil infrastructures. *Journal of Materials in Civil Engineering ASCE*, 15(3): 298–304.

Doebling, S.W., Farrar C.R., Prime M.B. & Shevitz D.W. 1998. A review of damage identification methods that

examine changes in dynamic properties. *Shock and Vibration Digest*, 30(2): 91–105.

Jansson, A. & Lundberg, B. 2007. Piezoelectric generation of extensional waves in a viscoelastic bar by use of a linear power amplifier: theoretical basis. *Journal of Sound and Vibration*, 306; 318–332.

Kim, S.D., In, C.W., Cronin, K.E., Sohn, H. & Harries, K. 2007. Reference-free NDT technique for debonding detection in CFRP-strengthened RC structures. *Journal of Structural Engineering ASCE*, 133(8): 1080–1091.

Limkatanyu, S. & Spacone, E. 2002 Reinforced concrete frame element with bond interfaces. I: Displacement-based, force-based, and mixed formulations. *Journal of Structural Engineering ASCE*, 128(3): 346–355.

Na, W.-B., Kundu, T. & Ehsani, M.R. 2003 Lamb waves for detecting delamination between steel bars and concrete. *Computer-Aided Civil and Infrastructure Engineering*, 18: 58–63.

Neild, S.A., Williams, M.S. & Mcfadden, P.D. 2002 Nonlinear behaviour of reinforced concrete beams under low-amplitude cyclic and vibration loads. *Engineering Structures*, 24: 707–718.

Rizzo, P., Sorrivi, E., Di Scalea, F.L. & Viola, E. 2007. Wavelet-based outlier analysis for guided wave structural monitoring: application to multi-wire strands. *Journal of Sound and Vibration* 307(1–2): 52–68.

Rose, J.L. 1999. *Ultrasonic waves in Solid Media*. Cambridge: Cambridge University Press.

Soh, C.K., Chiew, S.P. & Dong, Y.X. 1999. Damage model for concrete-steel interface. *Journal of Engineering Mechanics ASCE*, 125(8): 979–983.

Soh, C.K., Tseng, K.K.-H., Bhalla, S. & Gupta, A. 2000. Performance of smart piezoceramic patches in health monitoring of a RC bridge. *Smart Materials and Structures*, 9: 533–542.

Song, G., Gu, H., Mo, Y.L., Hsu, T.T.C. & Dhonde, H. 2007. Concrete structural health monitoring using embedded piezoceramic transducers. *Smart Materials and Structures*, 16: 959–968.

Worden, K., Manson, G. & Fieller, N.R.J. 2000. Damage detection using outlier analysis. *Journal of Sound and Vibration*, 229: 647–667.

Wu, F. & Chang, F.-K. 2006a. Debond detection using embedded piezoelectric elements in reinforced concrete structures. Part I: experiment. *Structural Health Monitoring*, 5(1): 5–16.

Wu, F. & Chang, F.-K. 2006b. Debond detection using embedded piezoelectric elements in reinforced concrete structures. Part II: Analysis and Algorithm. *Structural Health Monitoring*, 5(1): 17–28.

Yan, Y.J. & Yam, L.H. 2002. Online detection of crack damage in composite plates using embedded piezoelectric actuators/sensors and wavelet analysis. *Composite Structures*, 58: 29–38.

Zhu, X.Q. & Law, S.S. 2007. A concrete-steel interface element for damage detection of reinforced concrete structures. *Engineering Structures* 29(12): 3515–3524.